

An insight into the properties of ATiO_3 (A=Ti,Sr) materials for photovoltaic applications

Lynet Allan,^{1,*} Julius M. Mwabora,¹ and Musembi J. Robinson¹

¹*Department of Physics, School of Physical Sciences,
University of Nairobi, P.O.Box 30197-00100 Nairobi Kenya.*

(Dated: December 2, 2022)

One of the most active research areas in the world is the search for effective materials for use in the fields of optoelectronics and photovoltaics. The potential of materials like ATiO_3 (A=Ti,Sr) is yet largely untapped. Ab initio studies based on density functional theory (DFT) have been used to comprehensively explore the structural, electronic, elastic, and optical properties of Ti_2O_3 and SrTiO_3 . In this study, the ground state properties were computed with spin-orbit coupling (SOC), without spin-orbit coupling, and with the inclusion of Hubbard U parameter. Ti_2O_3 has been found to have electronic bandgaps of 0.059 eV without SOC, 0.131 eV with SOC, and 1.665 eV with Hubbard U. For SrTiO_3 , electronic bandgaps of 1.612 eV, 1.761 eV, and 2.769 eV have been obtained, respectively, without SOC, with SOC, and with Hubbard U. Ti-4d orbitals have been observed to dominate near the top of the valence band in each and every instance. SOC did not significantly affect the bandgaps and calculated lattice parameters for ATiO_3 (A=Ti,Sr). ATiO_3 (A=Ti,Sr) is mechanically stable at absolute zero pressure, according to the mechanical stability test. The optical band gap has been seen to increase when Hubbard U is taken into account. In general, the Hubbard U parameter enhances bandgap and optical property predictions. Ti_2O_3 and SrTiO_3 are good UV-Vis absorbers and appropriate for photovoltaic applications owing to the optical absorption coefficient curves being found to cover the ultraviolet to visible (UV-Vis) region.

Key words: Optical properties, Electronic and Elastic properties, DFT + U, Spin orbit coupling, ATiO_3 (A=Ti,Sr).

I. INTRODUCTION

The search for sustainable energy resources has become a key field of study due to rising global energy demands and the negative environmental pollution generated by the burning of fossil fuels¹⁻³. Titanium based oxides have been under investigation for the past few decades owing to their wide range of applications in environmental remediation and solar energy conversion,³⁻⁵. Titanium is one of the earth-abundant elements, and its oxides including titanium dioxide (TiO_2) and ATiO_3 (A= Ba,Ca,Fe) have gained significant attention for applications in technologies of electronics, energy conversion, catalysis, sensing, and so on⁶⁻⁹. Despite its large band gap, TiO_2 has been researched for its potential modification for solar harvesting^{10,11}. However, there hasn't been much focus on reduced TiO_2 compounds like Ti_2O_3 . Previously,¹² Yang Yang et al observed a cubic perovskite Ti_2O_3 unit cell made at room temperature at the Ti/SrTiO₃ interface, although they did not investigate the material's properties. We thoroughly investigate the structural, electrical, elastic, and optical properties of Ti_2O_3 and SrTiO_3 materials for photovoltaic applications as a result of this. Ti_2O_3 is Corundum structured and crystallizes in the trigonal R3c space group with Ti^{3+} atoms bonded to six equivalent O^{-2} atoms to form a mixture of edge, corner, and face-sharing TiO_6 octahedra as reported elsewhere¹³. Similarly, SrTiO_3 is (Cubic) Perovskite structured and crystallizes in the tetragonal I4/mcm space group with Sr^{2+} bonded to twelve O^{-2} atoms to form SrO_{12} cuboctahedra that share corners with twelve equivalent SrO_{12} cuboctahedra. In this

study, the stability and properties of these two compounds will be explored their suitability for use in solar harvesting applications. Most recently¹⁴, the properties of titanium oxynitride compounds $\text{Ti}_n\text{N}_2\text{O}_{2n-1}$ with n=3, obtained from pristine Ti_2O_3 , were investigated. Ti_2O_3 displayed metallic properties, yet it had been reported to have semi-conducting properties experimentally¹⁵. The failure of first-principles DFT to properly describe the electronic band gaps of strongly correlated materials, in which the electron-electron interaction has a significant impact, is a well-known problem². Many approaches to resolving this discrepancy have been proposed. The inclusion of the Hubbard model (DFT+U) in electronic structure calculations is one of them². The DFT+U method has been used for improved prediction of the gaps as well as to exhaustively determine the elastic and mechanical properties of the compounds. The study of the elastic properties such as elastic constants provides fundamental information on how these materials behave under external strain¹⁶. Besides this, the effect of spin orbit coupling (SOC) has also been analyzed. To the best of our knowledge, there are a few experimental reports in the literature on the properties of Ti_2O_3 and SrTiO_3 . Hence, this work aimed at investigating the properties of the two titanites containing Ti^{3+} ions with a specific focus on their suitability for use in photovoltaic applications. Specifically, we explore the structural, electronic, elastic, mechanical, and optical properties of Ti_2O_3 and SrTiO_3 compounds using the DFT method with SOC and Hubbard U effects. This study opens new doors towards some new titanite-based technologies. This paper is organized as follows: Sec.II

accounts for the technicalities that may be needed for future reproducibility in our computations. We offer detailed analysis of results and discussions in Sec.III. The structural properties of both Ti_2O_3 and SrTiO_3 with and without SOC effects are discussed in Sec.III A while the effect of SOC and Hubbard U on electronic Properties in Sec.III B. The elastic constants and mechanical properties of the compounds under study are outlined in Sec.III C. In Sec.III D, we discuss the optical properties of Ti_2O_3 and SrTiO_3 . Sec.IV outlines the conclusions of this work.

II. COMPUTATIONAL DETAILS

The structural, electronic, elastic, mechanical, and optical properties of Ti_2O_3 and SrTiO_3 compounds were computed within the DFT^{16,17} as implemented in the quantum espresso (QE) code¹⁸. The Ti_2O_3 and SrTiO_3 crystal structure input files were downloaded from the materials project database¹⁹ and the materials cloud²⁰ input generator implemented in QE was used to generate the PWscf input files for DFT calculations. The electron-ion interaction was denoted by using the projector augmented-wave function (PAW) method²¹. The Generalized Gradient Approximation (GGA) with the Perdew-Burke-Ernzerhof (PBE)²² was chosen to define the exchange-correlation effect of the electrons. The optimized cutoff energy of 50Ry and $6 \times 6 \times 4$ Monkhorst-Pack grid for Brillouin zone integration were used for the calculations. Geometry optimization was performed by computing the total energy per unit cell at several lattice constant values to obtain the ground state structural properties. Based on the optimized lattice constants, the elastic, electronic, and optical properties were calculated. The effects of spin orbit coupling (SOC) was included in the structural and electronic properties, while the well-known DFT underestimation problem was countered but the inclusion of Hubbard U correction on the electronic structure calculations. The choice of the effective Hubbard U values were pegged on earlier works done on same materials while assessing the impact of the inclusion of U on the lattice parameter(a_0) of the compounds.

III. RESULTS AND DISCUSSIONS

A. Structural Properties

Ti_2O_3 and SrTiO_3 compounds adopt trigonal and tetragonal crystal system as reported elsewhere²⁰. In order to achieve the equilibrium structure, one has to calculate the lattice parameter that minimizes the DFT total energy, the optimized crystal structures are shown in Figure 1. Table I shows bond strength for Ti_2O_3 and SrTiO_3 .

From Table I, the Ti-O bond is stronger than the Ti-Ti bond in Ti_2O_3 , while the Ti-O bond is stronger than

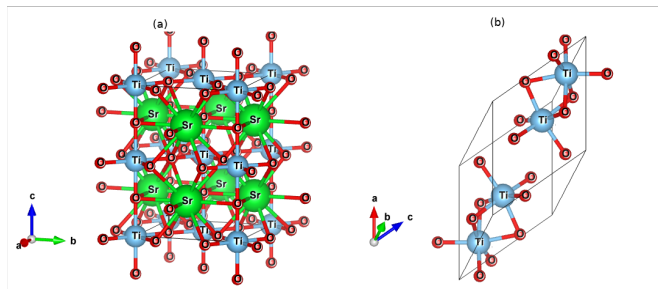


FIG. 1. Optimized Crystal structure for (a) SrTiO_3 and (b) Ti_2O_3 compounds

TABLE I. Bond lengths for Ti_2O_3 and SrTiO_3 compounds

Material	Bond	Bond length
Ti_2O_3	Ti-O	2.04
	Ti-Ti	2.37
SrTiO_3	Sr-Ti	3.41
	Sr-O	2.78
	Sr-Sr	3.95

both Ti-Sr and Sr-O bonds in SrTiO_3 . The Sr-Sr bond is the weakest with long bond lengths; this difference is attributed to the fact that the volume per atom tends to increase with the increase in atomic radius and therefore affects crystal lattice basis²³. The total energy at various lattice constant values is computed with SOC and without SOC effects are presented in figure 2 and figure 3 for Ti_2O_3 and SrTiO_3 compounds, respectively. Table II gives a summary of the calculated lattice parameters and other structural properties.

From figure 2 and figure 3, SOC did not have significant effects on the lattice parameters. However, when the data was fitted to Murnaghan's equation of state²⁴, minimum changes were noted on the equilibrium volume and ground state energies of the two compounds as indicated in table II

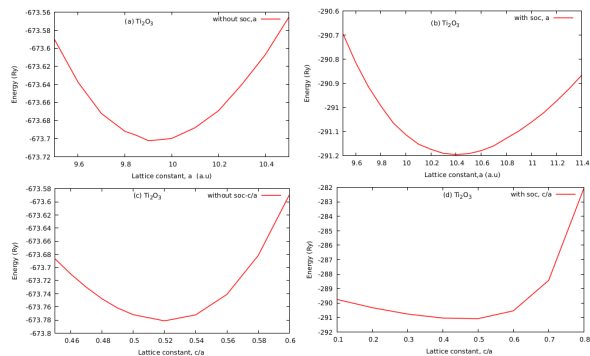
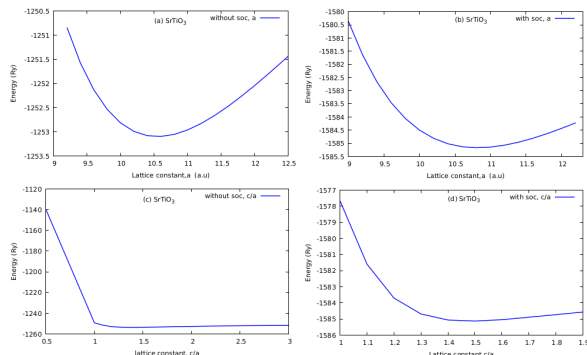


FIG. 2. Total energy versus lattice constants computed with and without SOC effects for Ti_2O_3 compound.

TABLE II. Effect of SOC on Structural properties of Ti_2O_3 and SrTiO_3 compounds

Structural Properties	Ti_2O_3		SrTiO_3	
	Without soc	With soc	Without soc	With soc
Lattice Parameters a_0 (a.u)	9.933	10.404	10.535	10.849
Lattice parameter c/a	0.520	0.571	1.353	1.403
Bulk modulus B_o (GPa)	166.4	137.0	217.1	218.2
Ground state energy				
E_o (ry)	-673.7	-291.1	-1253.07	-1585.16
Equilibrium volume				
V_o (a.u) ³	980.14	1126.09	1167.17	1277.00

FIG. 3. Total energy versus lattice constants computed with and without SOC effects for SrTiO_3 compound.

B. Effect of SOC and Hubbard U on Electronic Properties

The electronic band structures and projected density of states (PDOSs) of the Ti_2O_3 and SrTiO_3 compounds were computed by using the optimized crystal structures and presented on figure 4 and figure 5. The band structures were calculated in three stages; i) without SOC effects, ii) with SOC effect, and iii) with Hubbard U corrections. The choice of U values were pegged on the earlier works on the same materials by ref¹⁴ and ref²⁵ for Ti_2O_3 and SrTiO_3 , respectively. For Ti_2O_3 and SrTiO_3 , Hubbard $U=5$ eV and $U=7$ eV, respectively, proved to have no significant effects on the lattice constants and were therefore used for the band structure calculations.

The Ti_2O_3 and SrTiO_3 compounds have narrow bandgaps of Ti_2O_3 has been found to have electronic bandgaps of 0.059 eV and 1.612 eV, respectively, without SOC, 0.131 eV and 1.761 eV, respectively, with SOC, and 1.665 eV and 2.769 eV, respectively, with Hubbard U as seen in figures 4 and 5(a). The summary of the calculated bandgaps is tabulated in table III.

From the band structure calculations, SOC did not have significant effect on the bandgaps, however the DFT+U improved the prediction of the band gaps with respect to the experimental values. The maxima of the valence bands and the minima of the conduction bands occur at different symmetry points (Z- Γ) for Ti_2O_3 and

SrTiO_3 and (Γ -M) for SrTiO_3 in the Brillouin zone, implying that the two compounds are indirect bandgap semiconductors. The projected density of states, which describes the available states for electrons to occupy when projected on atomic orbitals were calculated. However, since the effects of SOC and without Hubbard U did not have significant impact on the types of dominant states in the PDOS, only the results of the PDOS without the effects of SOC and Hubbard U are presented in figures 4(b) and 5(b). The orbital contributions to the formation of valence bands and conduction bands are described by the PDOS in the energy region -4.5 eV to 4 eV. As illustrated in figure 4(b), the entire band structure is dominated with O-2p and Ti-4d orbitals, an indication that Ti_2O_3 exhibits semi metallic properties without Hubbard U effects, this is attributed to the well-known poor description of the electronic structure by the DFT method. The bands in the region -4.5 to -2.5 eV are majorly formed by O-2p while Ti-4d states forms the bands in the energy region of -1.0 eV to 4 eV in the Ti_2O_3 band structure shown in figure 5. In the case of SrTiO_3 compound (Figure 5(b)), the valence band is majorly formed by the O-2p states in the energy range of -4.5eV to Fermi level, while the conduction band is majorly formed by the Ti-4d orbitals.

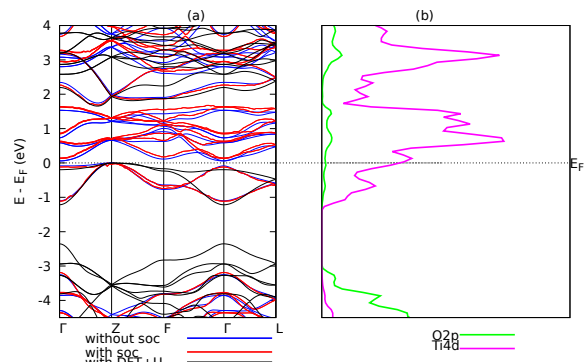
FIG. 4. The calculated (a) band structures of Ti_2O_3 compounds without SOC effects(blue), with SOC(red) and with DFT+U ($U=5$ eV) (black), (b)The PDOS for Ti_2O_3 compound without SOC and without DFT+U effects.

TABLE III. The calculated and experimental bandgaps

Materials	Calculated Band Gaps			Experimental gaps
	Without SOC	With SOC	With Hubbard U	
Ti ₂ O ₃	0.0598	0.1311	1.667 (U=5eV)	1.67 ¹²
SrTiO ₃	1.612	1.7612	2.769(U=7eV)	2.85 ²⁶

C. Mechanical and Elastic properties

The Ti₂O₃ and SrTiO₃ compounds adopt trigonal and tetragonal crystal structure featuring six independent elastic constants. The independent elastic constants for trigonal Ti₂O₃ are C_{11} C_{12} C_{13} C_{14} C_{33} C_{44} ²⁷. The necessary and sufficient conditions for trigonal elastic Ti₂O₃ stability is given by equation(1);

$$\begin{aligned}
 & C_{11} > |C_{12}|; C_{44} > 0; \\
 & C_{13}^2 < \frac{1}{2}C_{33}(C_{11} + C_{12}); \\
 & C_{14}^2 < \frac{1}{2}C_{44}(C_{11} - C_{12}) = C_{44}C_{66}; \\
 & C_{66} = \frac{1}{2}(C_{11} - C_{12})
 \end{aligned} \tag{1}$$

For Tetragonal SrTiO₃, the six independent elastic constants are C_{11} C_{12} C_{13} C_{14} C_{33} C_{44} and C_{66} ²⁷. The necessary and sufficient conditions for elastic stability of the tetragonal crystal system are ;

$$\begin{aligned}
 & C_{11} > |C_{12}|; C_{44} > 0; \\
 & 2C_{13}^2 < C_{33}(C_{11} + C_{12}); C_{66} > 0
 \end{aligned} \tag{2}$$

Table IV shows the calculated elastic constants for both the compounds, from the results, both the compounds meet the stability criteria, at DFT and DFT+U levels, and are therefore mechanically stable. The bulk modulus B, Young's modulus E, shear modulus G, Pugh's ratio B/G, and Poisson's ratio n are presented in table V.

Bulk modulus measures the resistance against volume change resulting from applied external pressure²⁸. Large B value predicts hard materials; thus, from the computed values of the bulk modulus, both Ti₂O₃ and SrTiO₃ are not hard materials. It is clear that for Ti₂O₃, DFT+U gives a more accurate prediction of the mechanical properties with reference to the values obtained (in table II) when lattice constants were fitted to Murnaghan's equation of state²⁹. Additionally, the bond lengths of the crystal structures are correlated to the size of the B. The shorter the bond lengths, the larger the B value³⁰. From the structural properties, the obtained bond lengths in Ti₂O₃ are shorter than those in the SrTiO₃ crystal structure thus the higher value of B in Ti₂O₃ compound by DFT calculations. The ductile (ionic) and brittle (covalent) nature of materials is determined by Pugh's ratio B/G and Poisson's ratio, n²⁸. The restriction for brittleness is B/G < 1.75; otherwise, the material is said to be ductile. In addition, the Cauchy pressure ($C_{12} - C_{44}$) also confirms the ductility and brittleness of materials. A positive value of the Cauchy pressure indicates ductility and brittleness otherwise. The critical value for the Poisson's ratio is 0.26, with materials having n as 0.26 exhibiting a ductile nature and brittleness otherwise. From the calculated values, all the three methods are consistent in classifying the materials as brittle. Poisson's ratio n 0.1, 0.25, and 0.33 for pure covalent, ionic, and metallic bonds, respectively,³⁰. Thus, we can conclude that Ti₂O₃ and SrTiO₃ compounds are ductile and strongly dominated by ionic character. The stiffness of a material is determined by applying Young's modulus value³⁰. The higher the value of E, the stiffer the material, therefore, SrTiO₃ compound is stiffer than Ti₂O₃.

D. Optical Properties

Optical properties of solids, which dependent on their band gap, are very interesting to know how the solid interacts with light. To highlight optical properties such as: reflection transmission and absorption, we need to calculate the dielectric function $\epsilon(\omega)$, which reflects the response of electrons in solid to electromagnetic irradiation. The dielectric function $\epsilon(\omega)$ is given by :

$$\epsilon(\omega) = \epsilon_1(\omega) + i\epsilon_2(\omega) \tag{3}$$

$\epsilon_1(\omega)$ and $\epsilon_2(\omega)$ are the real and the imaginary parts of the dielectric function. The real part is associated to the electronic polarizability of the material while the

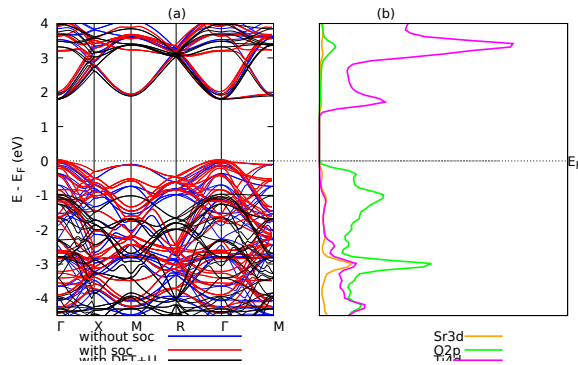


FIG. 5. The calculated (a) band structures of SrTiO₃ compounds without SOC effects (blue), with SOC(red) and with DFT+U (U=5 eV) (black), (b)The PDOS for SrTiO₃ compound without SOC and without DFT+U effects.

TABLE IV. Computed elastic constants C_{ij} (GPa) of Ti_2O_3 and SrTiO_3 compounds

Compound		C_{11}	C_{12}	C_{13}	C_{14}	C_{33}	C_{44}	C_{66}
Ti_2O_3	DFT	350.3	138.9	175.7	83.04	276.0	114.7	105.6
	DFT+U	285.3	102.1	113.4	3.073	228.4	121.5	91.6
SrTiO_3	DFT	338.3	110.6	105.7	-	351.6	116.5	122.3
	DFT+U	372.5	116.7	115.2	-	383.3	130.3	133.0

TABLE V. Mechanical properties of Ti_2O_3 and SrTiO_3 compounds

Compound		B	E	G	B/G	n
Ti_2O_3	DFT	217.0	250.2	95.7	2.26	0.31
	DFT+U	161.3	239.4	95.5	1.69	0.25
SrTiO_3	DFT	185.8	292.4	118.1	1.57	0.24
	DFT+U	202.5	322.9	130.8	1.54	0.23

imaginary part is correlated to the electronic absorption of material³¹. The real part and the imaginary parts describe, respectively, the dispersion and the absorption of the electromagnetic radiation by the medium which it crosses. The spectrum is calculated by summing the electric dipole operator matrix elements between the occupied and unoccupied wave functions over the Brillouin zone while respecting the selection rules. This is mainly connected with the electronic structures and characterizes the linear response of the material to electromagnetic radiation. It therefore governs the propagation behavior of radiation in a medium. The imaginary part of the dielectric function represents the electron transition between the valence and the conduction bands. The other optical properties like as: the reflectivity $R(\omega)$, the absorption $\alpha(\omega)$ and the refractivity $n(\omega)$, can be derived from $\epsilon_1(\omega)$ and $\epsilon_2(\omega)$. These are presented in Figure 6, 7 and 8 are computed by using the equations presented as follows^{4,31,32}:

$$\alpha(\omega) = \sqrt{2}\omega \left(\sqrt{\epsilon_1^2(\omega) + \epsilon_2^2(\omega)} - \epsilon_1(\omega) \right)^{1/2} \quad (4)$$

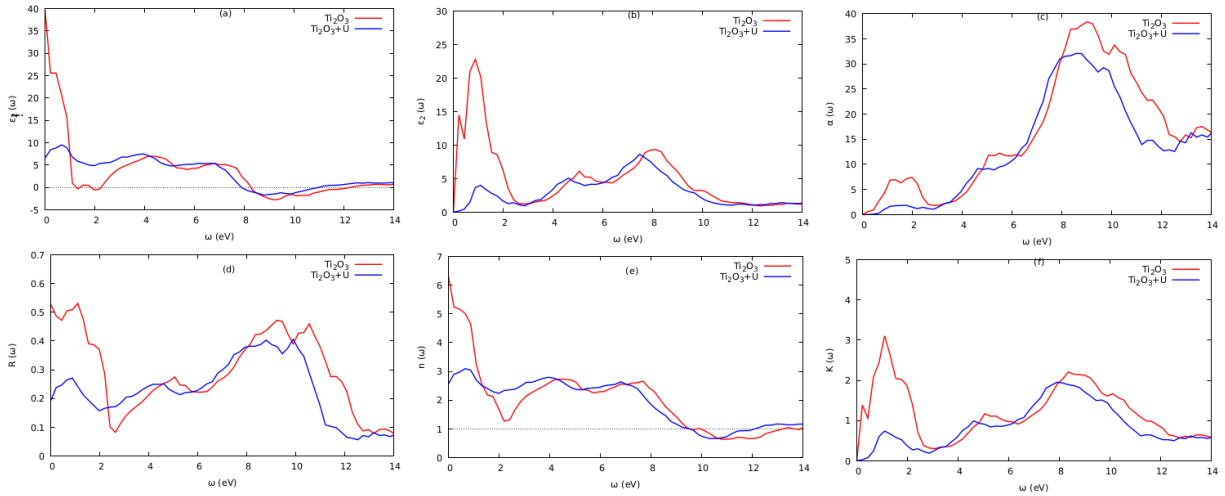
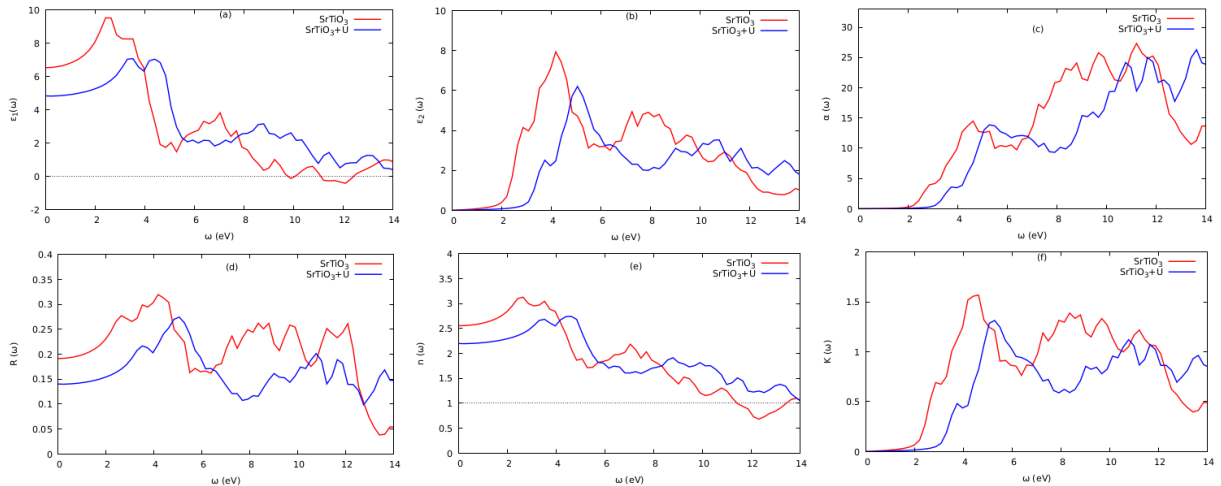
$$n(\omega) = \sqrt{2}\omega \left(\frac{\sqrt{\epsilon_1^2(\omega) + \epsilon_2^2(\omega)} - \epsilon_1(\omega)}{2} \right)^{1/2} \quad (5)$$

$$K(\omega) = \sqrt{2}\omega \left(\frac{\sqrt{\epsilon_1^2(\omega) + \epsilon_2^2(\omega)} - \epsilon_1(\omega)}{2} \right)^{1/2} \quad (6)$$

$$L(\omega) = \frac{\epsilon_2(\omega)}{\epsilon_1^2(\omega) + \epsilon_2^2(\omega)} \quad (7)$$

$$R(\omega) = \frac{(n-1)^2 + K^2}{(n+1)^2 + K^2} \quad (8)$$

The imaginary part ($\epsilon_2(\omega)$) of the dielectric wave function describes the photon absorption in crystalline materials¹³. The peaks in ($\epsilon_2(\omega)$) curves result from the electronic transitions from the valence to the conduction bands. The absorption onsets in $\alpha(\omega)$ curves refer to the materials bandgaps which lie within the visible region, <3.1 eV for Ti_2O_3 and SrTiO_3 compounds, and are consistent with the bandgaps from the band structure, an implication of strong inter-band transitions. This makes for Ti_2O_3 and SrTiO_3 compounds promising candidates for photovoltaic applications. Additionally, narrow bandgaps facilitate faster electron transitions as opposed to wide bandgaps⁴. The key feature of the ($\epsilon_1(\omega)$) curve is ($\epsilon_1(\omega)$ Energy=0), also referred to as the static value³². This static value is correlated to the material's refractive index as $n(\omega)$. Starting from Energy 0, the ($\epsilon_1(\omega)$) plot attained major peaks at low energy regions, <1.5eV and <2.7 eV for Ti_2O_3 and SrTiO_3 , respectively. The photon transmission persisted until the $\text{Re}(\omega)$ values became negative at energy regions of 8eV - 12eV. At this energy region, the incident photon radiations are assumed to be fully attenuated³³ and the compounds assert a metallic behaviour³⁴. From $n(\omega)$ curves, the calculated refractive indices obtained at zero energies are 2.3 (DFT+U) and 2.5 (without U) for SrTiO_3 and 2.5 (with Hubbard U) for SrTiO_3 . The major refractive index peaks for SrTiO_3 and Ti_2O_3 (with Hubbard U) reside within the visible region. Additionally, the Ti_2O_3 and SrTiO_3 were found to have high optical absorption in the energy range of 8eV-10eV and 10eV-12eV, respectively. The optical absorption coefficients of Ti_2O_3 and SrTiO_3 compounds cover the UV-Vis regions. The absorption coefficients calculated covered a wide range of the electromagnetic spectrum in the energy regions 2.0–13.5 eV; this demonstrates that these compounds can be utilized for photovoltaic applications. The materials' surface behaviour and energy loss by fast electrons entering a medium are determined by reflectivity and energy loss function, respectively³². The main peaks of the reflectivity curves are observed in the regions 6 eV -11 eV and 2 eV-6 eV for Ti_2O_3 and SrTiO_3 , respectively, the reflectivity decreased beyond this region. There was no significant absorption in the visible regions, as depicted in the loss spectrum for both compounds in figures 8(a) and 8(b). The major absorption peak occurred at higher energy regions 9.97–12.71 eV. The major absorption peak occurred at higher energy regions >12 eV and >10 eV for SrTiO_3 and Ti_2O_3 , respectively. The optical properties results obtained in this work are in agreement with the results obtained previously on the related materials^{4,31}.

FIG. 6. Optical Properties for Ti_2O_3 FIG. 7. Optical Properties for SrTiO_3

IV. CONCLUSION

We have studied the structural, electronic, elastic, mechanical, and optical properties of Ti_2O_3 and SrTiO_3 compounds using the DFT (with and without SOC effects), and DFT+U methods as implemented in the QE package. Interestingly, SOC did not have significant effects on the structural and electronic properties of the compounds. Equilibrium lattice constants of 9.93 a.u without SOC and 10.40 a.u with SOC were obtained for Ti_2O_3 compound, whereas for SrTiO_3 the calculated equilibrium lattice constants were 10.53 a.u and 10.84 a.u without SOC and with SOC, respectively. Ti_2O_3 was found to have electronic bandgaps of 0.059 eV without SOC and 0.131 eV with SOC while SrTiO_3 electronic bandgaps were 1.612 eV, and 1.761 eV, respectively, without SOC and with SOC. When the Hubbard U effects were in cooperated in the electronic structure calculations, the bandgaps for Ti_2O_3 and SrTiO_3 , were predicted as 1.665 eV and 2.769 eV, respectively. These

were in fairly good agreement with reported experimental results. The formation of the conduction band was primarily by Ti-4d, while the valence bands were dominated by O-2p orbitals in both compounds. Both Ti_2O_3 and SrTiO_3 were found to be mechanically stable at zero pressure, ductile, and ionic, thus their potentiality for resilient materials application, these properties were confirmed by DFT+U studies. Additionally, the optical properties of Ti_2O_3 and SrTiO_3 were improved by DFT+U studies. The calculated bandgaps, high refractive indices, high absorption coefficients, and wide energy coverage of the absorption coefficients spectra was mainly in the UV-Vis regions of the electromagnetic spectrum. This work suggests that Ti_2O_3 and SrTiO_3 compounds are suitable for photovoltaic applications.

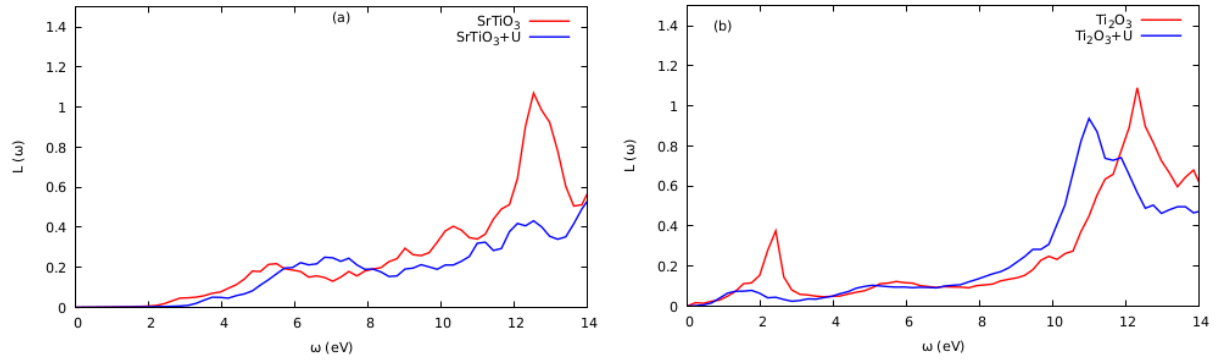


FIG. 8. Energy loss $L(\omega)$ for ATiO_3

V. ACKNOWLEDGMENTS

This work was supported by the Partnership for Skills in Applied Sciences, Engineering and Technology (PASET)—Regional Scholarship Innovation Fund (RSIF). The authors acknowledge the Centre for High-Performance Computing, CHPC, Cape for HPC resources.

VI. DATA AVAILABILITY

The source files and data will be assessed upon request from the authors.

VII. CONFLICTS OF INTEREST

The authors declare that they have no conflicts of interest.

-
- * Corresponding author: allanlynet3@students.uonbi.ac.ke
- ¹ A. Eddiouane, H. Chaib, A. Nafidi, M. Najjaoui, and T. Ait-Taleb, in *AIP Conference Proceedings*, Vol. 2056 (AIP Publishing LLC, 2018) p. 020005.
 - ² M. Samat, A. Ali, M. Taib, O. Hassan, and M. Yahya, *Results in physics* **6**, 891 (2016).
 - ³ T. Umebayashi, T. Yamaki, H. Itoh, and K. Asai, *Journal of Physics and Chemistry of Solids* **63**, 1909 (2002).
 - ⁴ M. Samat, A. Ali, M. Taib, O. Hassan, and M. Yahya, *Materials Today: Proceedings* **17**, 472 (2019).
 - ⁵ F. Giustino, *Materials modelling using density functional theory: properties and predictions* (Oxford University Press, 2014).
 - ⁶ B. Zhang, J. Sun, H. Katz, F. Fang, and R. Opila, *ACS applied materials & interfaces* **2**, 3170 (2010).
 - ⁷ O. L. Anderson, *Journal of Physics and Chemistry of Solids* **24**, 909 (1963).
 - ⁸ S. N. R. Inturi, T. Boningari, M. Suidan, and P. G. Smirniotis, *Applied Catalysis B: Environmental* **144**, 333 (2014).
 - ⁹ Y. Li, Y. Yang, X. Shu, D. Wan, N. Wei, X. Yu, M. B. Breese, T. Venkatesan, J. M. Xue, Y. Liu, *et al.*, *chemistry of materials* **30**, 4383 (2018).
 - ¹⁰ A. Fahmi, C. Minot, B. Silvi, and M. Causa, *Physical Review B* **47**, 11717 (1993).
 - ¹¹ Y. Zhang and D. S. Kilin, *International Journal of Quantum Chemistry* **112**, 3867 (2012).
 - ¹² Y. Li, *Investigation of Titanium Sesquioxide Ti2O3: Synthesis and Physical Properties*, Ph.D. thesis (2016).
 - ¹³ Y. Guo, S. J. Clark, and J. Robertson, *Journal of Physics: Condensed Matter* **24**, 325504 (2012).
 - ¹⁴ L. Allan, G. O. Amolo, J. Mwabora, and S. Mureramanzi, *arXiv preprint arXiv:2201.00212* (2022).
 - ¹⁵ Y. Aoki, M. Sakurai, S. Coh, J. R. Chelikowsky, S. G. Louie, M. L. Cohen, and S. Saito, *Physical Review B* **99**, 075203 (2019).
 - ¹⁶ K. Burke *et al.*, Department of Chemistry, University of California, 40 (2007).
 - ¹⁷ W. Kohn and L. J. Sham, *Phys. Rev.* **140**, A1133 (1965).
 - ¹⁸ P. Giannozzi, S. Baroni, N. Bonini, M. Calandra, R. Car, C. Cavazzoni, D. Ceresoli, G. L. Chiarotti, M. Cococcioni, I. Dabo, A. D. Corso, S. de Gironcoli, S. Fabris, G. Fratesi, R. Gebauer, U. Gerstmann, C. Gougoussis, A. Kokalj, M. Lazzeri, L. Martin-Samos, N. Marzari, F. Mauri, R. Mazzarello, S. Paolini, A. Pasquarello, L. Paulatto, C. Sbraccia, S. Scandolo, G. Sclauzero, A. P. Seitsonen, A. Smogunov, P. Umari, and R. M. Wentzcovitch, *Journal of Physics: Condensed Matter* **21**, 395502 (2009).
 - ¹⁹ A. Jain, S. P. Ong, G. Hautier, W. Chen, W. D. Richards, S. Dacek, S. Cholia, D. Gunter, D. Skinner, G. Ceder, *et al.*, *APL materials* **1**, 011002 (2013).
 - ²⁰ L. Talirz, S. Kumbhar, E. Passaro, A. V. Yakutovich, V. Granata, F. Gargiulo, M. Borelli, M. Uhrin, S. P. Huber, S. Zoupanos, *et al.*, *Scientific data* **7**, 1 (2020).

- ²¹ G. Kresse and D. Joubert, *Phys. Rev. B* **59**, 1758 (1999).
- ²² J. P. Perdew, K. Burke, and M. Ernzerhof, *Phys. Rev. Lett.* **77**, 3865 (1996).
- ²³ E. Mooser and W. Pearson, *Canadian Journal of Physics* **34**, 1369 (1956).
- ²⁴ B. J. Morgan and G. W. Watson, *The Journal of Physical Chemistry C* **114**, 2321 (2010).
- ²⁵ A. A. Adewale and A. Chik, *INTERNATIONAL JOURNAL* **12**, 11 (2019).
- ²⁶ K. Van Benthem, C. Elsässer, and R. French, *Journal of applied physics* **90**, 6156 (2001).
- ²⁷ D. Chung and W. Buessem, *Journal of Applied Physics* **38**, 2535 (1967).
- ²⁸ L. Allan, W. M. Mulwa, R. J. Musembi, and B. O. Aduda, *arXiv preprint arXiv:2204.03759* (2022).
- ²⁹ F. Murnaghan, Proceedings of the national academy of sciences of the United States of America **30**, 244 (1944).
- ³⁰ G. S. Manyali, *Ab-initio study of elastic and structural properties of layered nitride materials*, *Ph.D. thesis*, University of the Witwatersrand, Faculty of Science, School of Physics (2012).
- ³¹ F. Aslam, B. Sabir, and M. Hassan, *Applied Physics A* **127**, 1 (2021).
- ³² A. Arbab, *Optik* **194**, 163067 (2019).
- ³³ G. Murtaza and I. Ahmad, *Physica B: Condensed Matter* **406**, 3222 (2011).
- ³⁴ G. Murtaza, I. Ahmad, B. Amin, A. Afaq, M. Maqbool, J. Maqssod, I. Khan, and M. Zahid, *Optical Materials* **33**, 553 (2011).